The Pennsylvania State University

The Graduate School

Department or Architectural Engineering

THERMAL AND VENTILATION PERFORMANCE OF COMBINED PASSIVE CHILLED BEAM – DISPLACEMENT VENTILATION SYSTEMS

A Thesis in

Architectural Engineering

by

Wenyu Shan

Submitted in Partial Fulfillment
of the Requirements
for the Degree of

Master of Science

May 2017

The thesis of Wenyu Shan was reviewed and approved* by the following:

Donghyun Rim
Assistant Professor of Architectural Engineering
Thesis Advisor

William Bahnfleth
Professor of Architectural Engineering

James Freihaut
Professor of Architectural Engineering

Richard Mistrick
Associate Professor of Architectural Engineering
Graduate Program Chair of Architectural Engineering

*Signatures are on file in the Graduate School

ABSTRACT

Chilled beam systems provide sensible cooling in the occupied space using chilled water flowing through modular heat exchangers mounted to a ceiling. Chilled beam systems can achieve cooling energy saving compared to all-air system due to greater thermal energy delivered by the chilled water than air, and thus are well-suited for spaces with relatively large sensible cooling loads as an energy-saving method. The objective of the present study is to study air conditioning performance of combined passive chilled beam (PCB) - displacement ventilation (DV) systems. Using computational fluid dynamics (CFD) simulations, the amount of sensible cooling by PCB and its impacts on ventilation effectiveness and thermal comfort in a typical office room are investigated. Simulations for combined PCB-DV system under different load and ventilation conditions are also conducted to study the system performance. The study results reveal that the thermal and ventilation performance can vary significantly with type of ventilation strategy, type of air supply diffuser, PCB cooling output and supply air temperature. However, arrangement of heat sources has a marginal effect on the performance of combined PCB-DV systems. With a PCB cooling output of 50% of the total cooling load and the supply air temperature of 19-20 ℃, the combined PCB-DV system can achieve the best performance in terms of energy use, ventilation effectiveness, and occupant thermal comfort.

Keywords: air conditioning, mixing ventilation, displacement ventilation, computational fluid dynamics, ventilation effectiveness, thermal comfort

TABLE OF CONTENTS

LIST OF FIGURES

LIST OF TABLES

ACKNOWLEDGEMENTS

I would like to thank my advisor, Dr. Donghyun Rim at Penn State University for his guidance and support over the last two years. Dr. Rim gave me a lot of help on both academic study and personal life.

I would like to thank my committee members, Dr. William Bahnfleth and Dr. James Freihaut at Penn State University for their suggestions on this paper. Without their helpful opinions, this study could not have been successfully conducted.

I would also like to thank all my friends who kept encouraging and inspiring me to challenge and conquer the problems and difficulties.

Finally, I want to thank my parents who is the constant source of support, encouragement and inspiration during my academic and daily life. I could never have finished this paper without you.

Chapter 1

Introduction

A chilled beam system is an air conditioning system designed for buildings with a relatively large sensible cooling load ratio compared to conventional all-air system. Chilled beams are generally mounted to ceilings in an occupied zone and provide chilled water flowing through the coils. This cooling strategy receives increasing attention as an energy-saving method because chilled beams can deliver larger thermal energy at higher chilled water supply temperature compared to the conventional all-air system.

Passive chilled beam

Chilled beams are mainly classified into two types: passive and active. Passive chilled beam (PCB) systems provide cooling to an occupied space mainly based on the convection between the chilled beam coil surfaces and the indoor air. In this case, chilled water passes through the coils typically at temperature from 14 to 18 ℃ with a mass flow rate from 0.02 to 0.2 kg/s [1]. The cooling output of PCB is in a range of 20-40 W/m·K with the convective to radiant heat transfer ratio of 50:50 for hidden beams and 85:15 for exposed beams [2]. However, as a PCB system only provides space air conditioning without ventilation, it is generally combined with an additional ventilation (e.g. displacement and mixing ventilation). On the other hand, active chilled beam (ACB) systems supply conditioned air through the chilled beams and induce room air moving through the beams. Due to this forced convection, the cooling output of ACB is around 100-200 W/m·K, which is higher than that of PCB [2]. Typical supply air temperature

from ACB ranges between 18 to 19 ℃, and the mixing ratio of supply air to outdoor air can be as high as 6: 1 [3].

PCB and ACB systems share some common advantages compared with other conventional HVAC systems. They can employ warmer chilled water temperature for cooling, which improves the efficiency of chillers. The mechanical service space requirements for the chilled beam systems can be modest, helping reduce the construction and maintenance cost [3]. Chilled beam systems also have large potential for fan energy saving. Although PCB systems generally provide smaller cooling output than ACB systems, PCB systems can achieve larger fan energy saving because ACB systems still need higher system static pressure for air induction [3]. Furthermore, PCB systems are superior in silent operation and high-quality air supply due to the separation of air conditioning from outdoor air ventilation.

Several experimental studies have reported cooling characteristics of PCB systems. Kosonen et al. [4] have found the location and intensity of heat loads have a significant effect on the indoor air distribution with PCB systems. Fredriksson and Sandberg [5] studied the effect of a false ceiling on the cooling performance of the PCBs, and reported notable impacts of return opening location and area. Nelson et al. [6] reported that the effect of indoor heat source arrangement on cooling energy delivered by PCB based on experiments with PCB in a climatic chamber.

Design of a PCB system can be combined with displacement ventilation (DV) that supplies ventilation air in a conditioned zone through a supply diffuser located close to the floor. In this case, supply air is heated by indoor heat sources (e.g. occupants, electrical equipment, lights), rises due to buoyancy and is finally exhausted at ceiling height. In general, DV yields higher ventilation effectiveness in the occupied zone compared to mixing ventilation (MV) that provides supply air at ceiling level [7, 8]. Based on the working principles, it appears that combined PCB and DV system can provide opportunities to save cooling energy while improving

indoor air quality and thermal comfort. However, these two systems may impair the benefits of each. For example, overhead PCBs produce downward-moving plumes that interfere with the upward flow of DV. Few published studies have examined ventilation and thermal performances of combined PCB-DV systems. So, parametric analysis is required to find out the characteristics of combined PCB-DV system in terms of ventilation and thermal performances.

Study objectives

Based on the background, a numerical evaluation was performed based on computational fluid dynamics (CFD) simulation, with the following three specific objectives:

1) Investigate temperature and air flow pattern of combined PCB-DV systems.

2) Study ventilation effectiveness and thermal comfort associated with operating conditions of combined PCB-DV systems in a typical office room.

3) Examine optimal cooling output conditions of combined PCB-DV systems that maximize the benefits of both PCB and DV without having them interfere with each other.

Chapter 2

Research Methods

Computational fluid dynamics (CFD) modeling is useed to examine the ventilation and thermal performance of PCB systems. CFD modeling can provide detailed information of a non-uniform air distribution in a descriptive manner compared to analytical model or laboratory and field measurements. However, the accuracy and reliability of CFD modeling results must be carefully validated and verified [11]. In the present study, a CFD model has been constructed and validated with a full-scale measurement of air temperature and velocity profiles in a chamber with DV [8]. As for the model verification, Grid Convergence Index (GCI) is estimated to evaluate uncertainty due to discretization. The mass and energy conservation are carefully checked to make sure that the simulation results are accurate enough to analyze the real-world scenarios. Then the validated and verified CFD model is used further to perform parametric analyses that evaluate thoroughly the performance of combined PCB-DV system.

CFD model validation of DV system

The CFD validation is based on a full-scale experiment performed in a climate chamber by Kobayashi and Chen [8]. This chamber experiment simulates an office, equipped with two occupant simulators, two PCs, two desks, four ceiling lamps, one box, two floor swirl diffusers and one exhaust. Table 2-1 lists the detailed location, size and load intensity of each component

in this experiment. Figure 2-1 shows the configuration of the office room and nine positions for monitoring temperature and air velocity.

Table 2-1. Location, size and load intensity of each component in the test chamber

Objects	Size (m)			Location (m)			Heat Load (W)	
	Length	Width	Height	x	y	z	Conv.	Rad.
Room	5.16	3.65	2.27	0	0	0		
Window		3.35	1.16	5.16	0.15	0.94	* Surface temp. 34 ℃	
Diffuser 1	0.2	0.2		1.82	1.82	0		
Diffuser 2	0.2	0.2		3.84	1.82	0		
Exhaust	0.45	0.45		2.37	1.61	2.27		
Occupant 1	0.4	0.35	1.1	1.98	0.85	0	31.5	43.5
Occupant 2	0.4	0.35	1.1	3.13	2.45	0	31.5	43.5
PC 1	0.4	0.4	0.4	1.98	0.1	0.75	97.65	10.85
PC 2	0.4	0.4	0.4	3.13	3.15	0.75	97.65	10.85
Desk 1	2.23	0.75	0.75	0.35	0	0.75		
Desk 2	2.23	0.75	0.75	2.93	2.9	0.74		
Box 1	0.95	0.58	1.24	4.21	0	0		
Ceiling lamp 1	0.2	1.2	0.15	1.03	0.16	2.18	22.44	45.56
Ceiling lamp 2	0.2	1.2	0.15	3.61	0.16	2.18	22.44	45.56
Ceiling lamp 3	0.2	1.2	0.15	1.03	2.29	2.18	22.44	45.56
Ceiling lamp 4	0.2	1.2	0.15	3.61	2.29	2.18	22.44	45.56

Source: Table 2, Floor-supply displacement ventilation in a small office, Kobayashi, N. and Chen, Q.

(a) 3D view

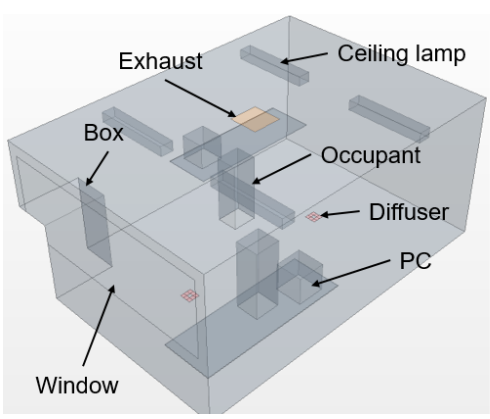

(b) Top view

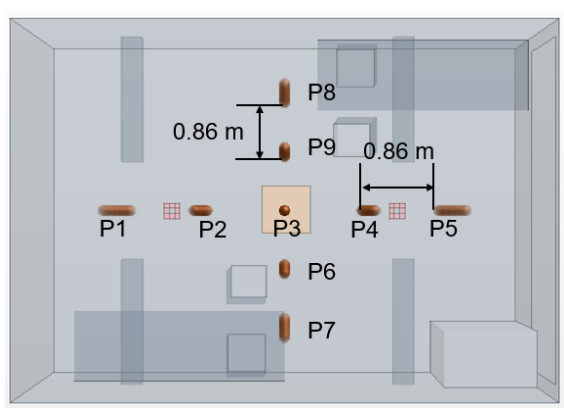

Figure 2-1. Office space configuration in the test chamber & the location of nine measuring positions: (a) 3D view; (b) top view

The room has two round-shape DV diffusers with a radius of 0.1m with a supply air temperature of 19 °C. In this study, the round diffusers are simplified to nine small square cells, similar to the approach of Kobayashi and Chen [8] (see Figure 2-2). Each of the nine cells simulate air swirl with the airflow direction angled at 60º to the floor plane [11]. The side length of each cell is 0.06 m, which gives a total supply area of 0.032 m^2. The supply velocity is 0.73 m/s that corresponds to an air exchange rate of 4 h^{-1}.

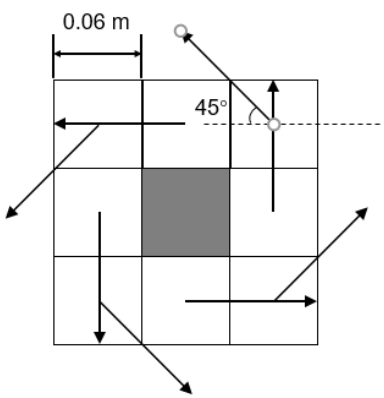

Figure 2-2. Description of the momentum method to simulate floor swirl diffuser

The computational grid of the CFD model is established based on polyhedral meshing scheme. The polyhedral mesher can minimize the number of generated cells while maintain the numerical accuracy [13]. To capture the heat and mass transfer in the domain accurately, the minimum size of mesh is 0.02 m around sensitive regions such as heat sources, air supply inlet, and exhaust. The minimum grid size is 0.025 m for the other regions. This condition generates around 400,000 grid cells in the computational domain.

As for turbulence model selection, SSN k-ω model is employed to simulate the indoor turbulent flow, as a previous CFD study shows that this model succeeded in reproducing the thermal plume structure and associated thermal stratification with DV systems, while other k-ε models yield lower accuracy [9]. Ideal gas and gravity models are considered to simulate the buoyancy effect due to the temperature gradient around heat sources.

Figure 2-3 presents the measured and simulated normalized temperature (TEM) and velocity of magnitude in the climate chamber. TEM is defined as a dimensionless value to indicate the vertical temperature profile in Equation (2-1):

$$TEM = \frac{T - T_{supply}}{T_{exhaust} - T_{supply}} \tag{2-1}$$

Three vertical temperature profiles at locations P3, P5 and P9 are chosen to compare the measurement and simulation (see Figure 2-1 (b)). The reason for the choice of these three locations is that they represent three types of regions: below the air exhaust (P3), close to the floor diffuser (P5) and close to the indoor heat source (P9). Figure 2-3 compares the temperature and velocity profiles at the three locations between the measurement and simulation. Figure 2-3 (a-c) illustrate that temperature goes up with the elevation, creating a thermal stratification. The agreements between the measured and simulated temperature are within 5% when the height > 0.5 m. However, the temperature difference is larger at the ground level, perhaps due to non-uniform temperature distribution on the floor surface in the experiment. However, the largest deviation of temperature is within 10% at the floor level while it is smaller than 5% for heights > 0.5 m.

Figure 2-3 (d-f) show that air velocity in the space is always smaller than 0.1 m/s, except the regions near the supply air diffusers and ceiling exhaust. The difference in velocity magnitude between the measured and simulated velocity are within 0.05 m/s for pole 3 and 9, while the

difference is larger for pole 5 (> 0.05 m/s). Nevertheless, the measurement uncertainty of anemometers used in the experiment is around 0.05 m/s when the velocity magnitude is lower than 0.1 m/s [8]. Based on the comparison of temperature and velocity profiles (Figure 2-3), CFD simulation and measurement results do not match perfectly; however, the results show that CFD simulation can provide insights into thermal stratification and velocity distribution due to DV with a reasonable accuracy.

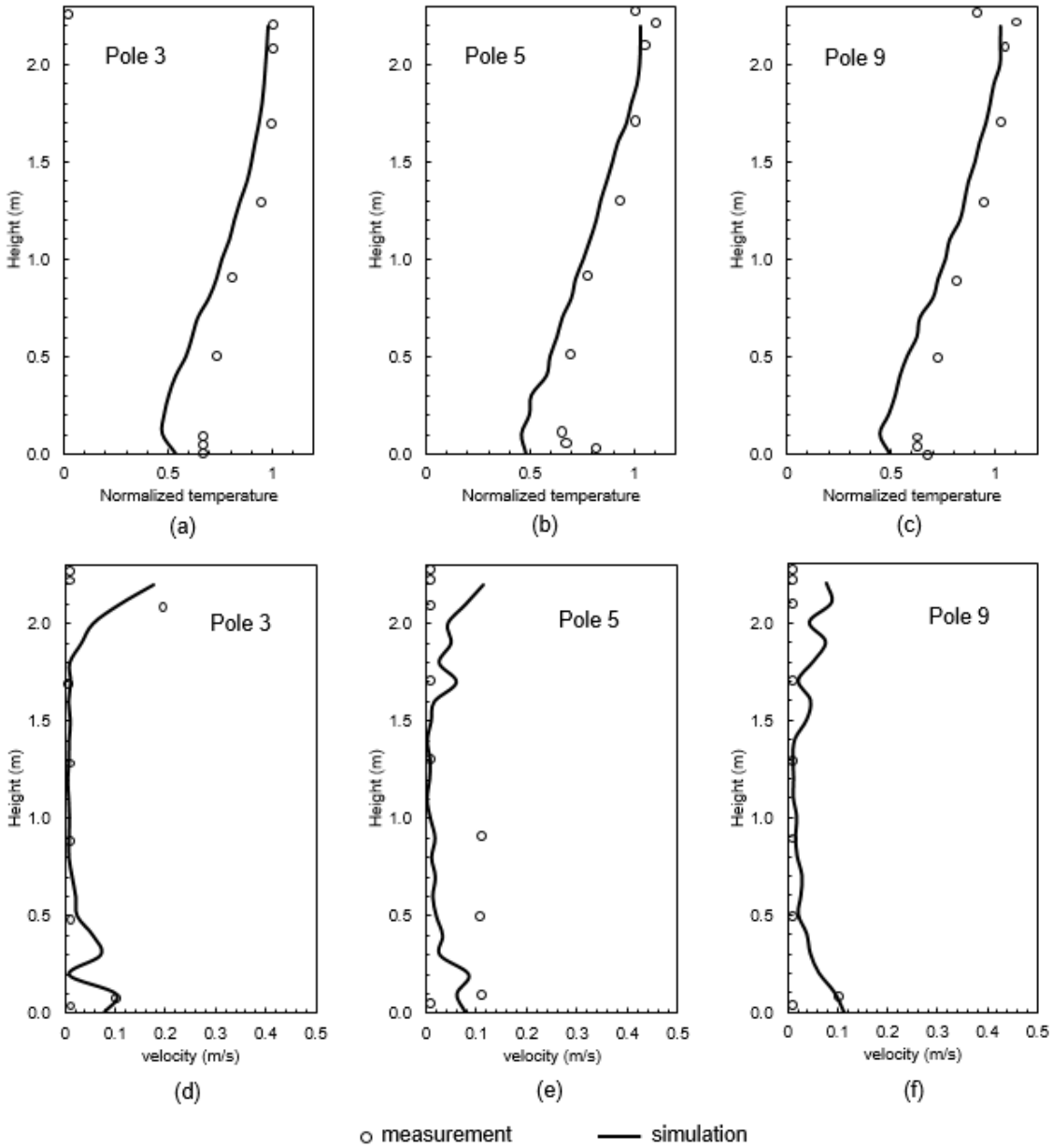

Figure 2-3. Comparison between measurement and simulation: vertical profiles of normalized temperature (a-c) and velocity (d-f) at three locations

Parametric analyses of combined PCB-DV system

Physical model

Using the validated CFD model, a typical office room with a combined PCB-DV system is simulated (see Figure 2-4). The simulated room has dimensions of 6 m × 4 m × 3 m (length × width × height). This model involved four seated occupants, two lights, four desktop computers, one office desk, and a window with a size of 3.2 m × 1.6 m.

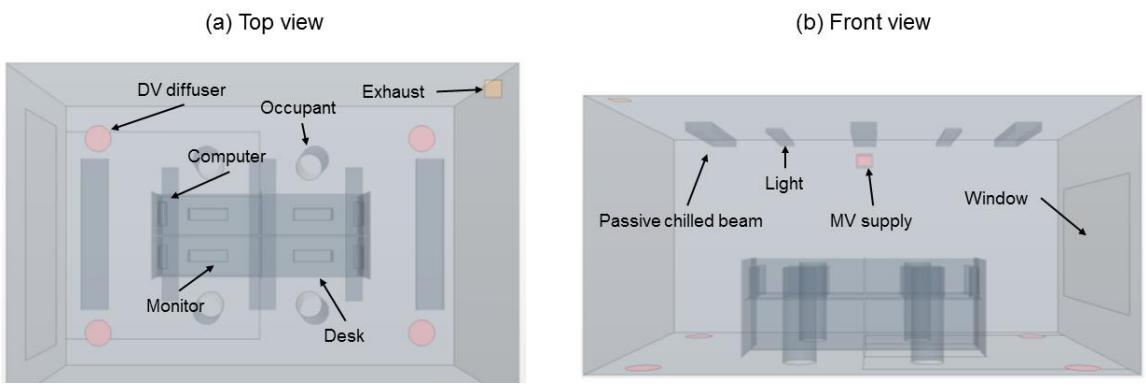

Figure 2-4. Office room configuration for parametric analyses: (a) top view; (b) front view

Three passive chilled beams are located near the ceiling with the size of 1.8 m × 0.32 m × 0.11 m (length × width × height) for each. The chilled beams are constructed as a solid cuboid 0.43 m away from the ceiling. The cooling output of each passive chilled beam is treated as a constant heat sink. Figure 2-5 shows the geometry and location of the three passive chilled beams.

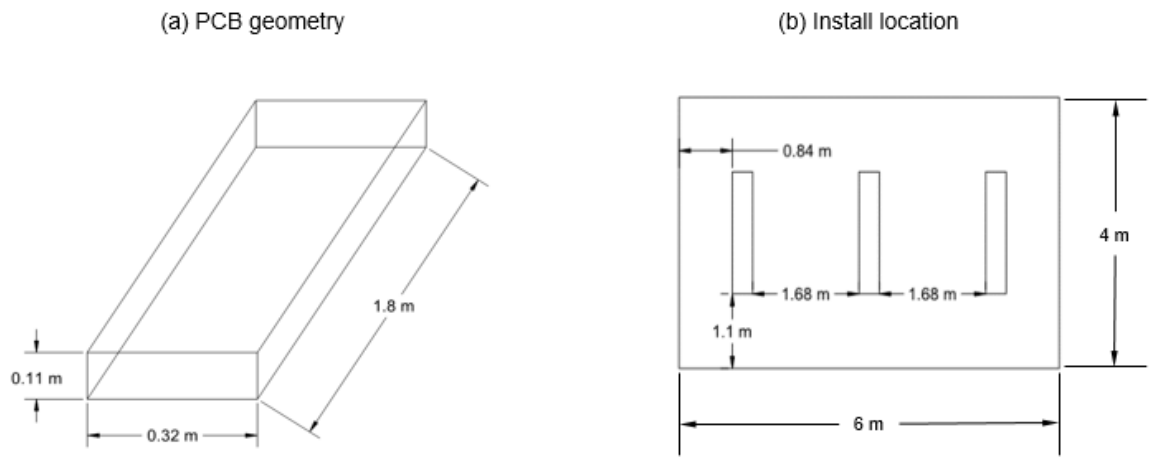

Figure 2-5. Geometry and location of passive chilled beams: (a) PCB geometry; (b) install location (top-view)

For the simulated office space, the total heat gain consists of the internal heat gain from indoor occupants, computers and lights and fenestration heat gain. The heat gain from each heat source is separated to convective and radiative portion. The internal heat load follows the 2013 ASHRAE Handbook, while the fenestration load is determined based on previous research [12]. The values of total, radiative and convective heat loads for each component are provided in Table 2-2. For indoor heat sources, the radiative heat is assumed to be absorbed by all wall surfaces (i.e. four side walls, ceiling and floor). For the fenestration load, the radiative heat is split into the window surface load and solar radiation on the floor near the window. In the CFD model, the heat flux for the sidewalls, ceiling and floor (away from the window) is 3.76 W/m^2, while the fluxes for the window and the floor near the window is 63.28 and 30.92 W/m^2, respectively. The unit heat load is 58.4 W/m^2, which is similar to the design values used in earlier studies [14, 15].

Table 2-2. Internal heat loads due to heat sources in the simulated office

Load Type	Sen. Heat (W)	Rad. (%)	Con. (%)	Number	Heat Load (W)
Occupant	75	58	42	4	300
Monitor	30	40	60	4	120
Desktop Computer	65	10	90	4	260
Light	100	67	33	2	200
Window Surface Load	324	0	100	1	324
Floor Radiation	198	0	100	1	198

To evaluate the effect of ventilation strategy, the MV system combined with PCB is also simulated with an air exchange rate of 4 h^{-1}. For the MV system, the supply air is provided through the side wall diffuser at ceiling height with a face velocity of 4 m/s to facilitate coanda effect.

CFD model grid and turbulence modeling

Using the same mesh setting with the validated model, the CFD model for parametric analyses is established based on polyhedral meshing scheme. The minimum size of mesh is 0.02 m around heat sources, air supply inlet and exhaust while the minimum grid size is 0.025 m for the other regions. The average y^+ values of the wall-adjacent cells (i.e. dimensionless wall distance) are 6 for indoor heat sources (e.g. occupants, lights, computers) and 8 for building enclosure including the window. The range is acceptable to predict turbulent flow in the wall boundary layer [16]. This condition generates around 900,000 grid cells in the computational domain.

Similarly, the turbulence model for parametric analyses is also based on the validated model. SSN k-ω, ideal gas and gravity models are employed in the CFD model for parametric analysis. Along with the ideal gas model, a multiple-gas model is used to simulate transport of a

passive tracer gas (sulfur hexafluorides, SF_6) and calculate the age-of-air and ventilation effectiveness.

CFD model verification

Verification is a process to determine if the model is capable of solving a system of coupled differential equations with a set of initial and/or boundary conditions, and reproduces the exact solution when sufficiently fine grid resolution is employed [17]. In the present study, verification of the CFD model is performed based on two main tasks as follows. First mass and energy conservation is evaluated to ensure the quality of the simulation results. Second, the discretization error is estimated based on the study of grid convergence index (GCI). GCI is calculated to quantify the results of grid convergence and provide an error range associated with grid refinement. The GCI can be calculated as indicated in Equation (2-2) [17]:

$$GCI^{21} = \frac{1.25}{(r_{21})^p - 1}\left|\frac{f_1 - f_2}{f_1}\right| \tag{2-2}$$

where f_1 and f_2 is the quantity of interest on the grid 1 and grid 2, r_{21} is the grid refinement factor that equals the ratio of the finest cell size between two grids (coarse to fine), and p is the order of convergence. In this study, three cell sizes (0.02 m, 0.06 m, 0.1 m), applied to the vicinity of heat sources, diffusers and exhaust, are chosen to calculate GCI. The quantity of interest, f, is the average velocity of magnitude for the 8 L volume of air located 0.2 m above an occupant simulator (P1) (see Figure 2-6). This quantity is one of the most sensitive parameter to the intensity of thermal plume in displacement ventilation [21]. The order of convergence, p, is determined using the equations found in Celik et al. [17]. Two GCI values (GCI^{21} and GCI^{32})

from three levels of grid are calculated to check if the discretization errors decrease with grid refinement.

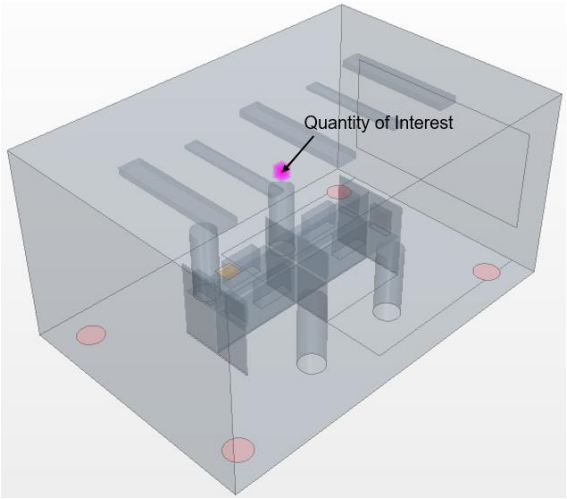

Figure 2-6. Location of quantity of interest in the office space

Simulation cases for parametric analysis

Using the verified and validated model, this study performs further parametric analyses to examine the impact of the following input parameters on the thermal comfort and ventilation effectiveness in a typical office room. A total of 17 cases are simulated to investigate the ventilation and thermal performances of PCB systems (see Table 2-3).

Table 2-3. Test cases for parametric analyses

Case	Ventilation strategy	PCB cooling output (W/m^2)	Air supply diffuser type	Supply air temp. (°C)	Heat source arrangement
1	MV	13	Sidewall grille	17	Arr_0
2	MV	19	Sidewall grille	17	Arr_0
3	MV	25	Sidewall grille	17	Arr_0
4	MV	19	Linear slot diffuser	17	Arr_0
5	DV	13	Floor-supply diffuser	17	Arr_0
6	DV	16	Floor-supply diffuser	17	Arr_0
7	DV	19	Floor-supply diffuser	17	Arr_0
8	DV	22	Floor-supply diffuser	17	Arr_0
9	DV	25	Floor-supply diffuser	17	Arr_0
10	DV	28	Floor-supply diffuser	17	Arr_0
11	DV	31	Floor-supply diffuser	17	Arr_0
12	DV	19	Floor-supply diffuser	18	Arr_0
13	DV	19	Floor-supply diffuser	19	Arr_0
14	DV	19	Floor-supply diffuser	20	Arr_0
15	DV	19	Wall-mounted diffuser	17	Arr_0
16	DV	19	Floor-supply diffuser	17	Arr_1
17	DV	19	Floor-supply diffuser	17	Arr_2

The parametric analysis mainly focuses on impacts of the 5 parameters as the following 5 groups:

1) Ventilation Strategy: MV and DV system are compared with the same PCB cooling output (cases 2 vs. case 7). The cooling output of each beam is kept at 150 W. The sidewall air slot of the MV system is mounted 0.3 m away from the ceiling with a size of 0.2 m × 0.1 m. In the DV system, four underfloor diffusers are placed in the corners of the room (0.6 m away from the sidewalls), each with a radius of 0.2 m.

2) Air Supply Diffuser: To find the effect of air supply diffuser on the performance of the PCB systems, two different diffusers are simulated for the MV and DV system. For the combined PCB-MV system, the sidewall grille (case 2) is compared with the linear slot diffuser (case 4, see Figure 2-7 (a)) at ceiling height, while for the combined PCB-DV system, the floor-supply diffusers (case 7) are compared with the wall-mounted diffusers (case 15), which are arranged in

the four corners of the room (see Figure 2-7 (b)). The size of the linear slot diffuser is 0.8 m × 0.05 m which provides a downward air at 2 m/s. The wall-mounted diffuser has a supply velocity of 0.16 m/s, which is the same with the floor-supply diffuser.

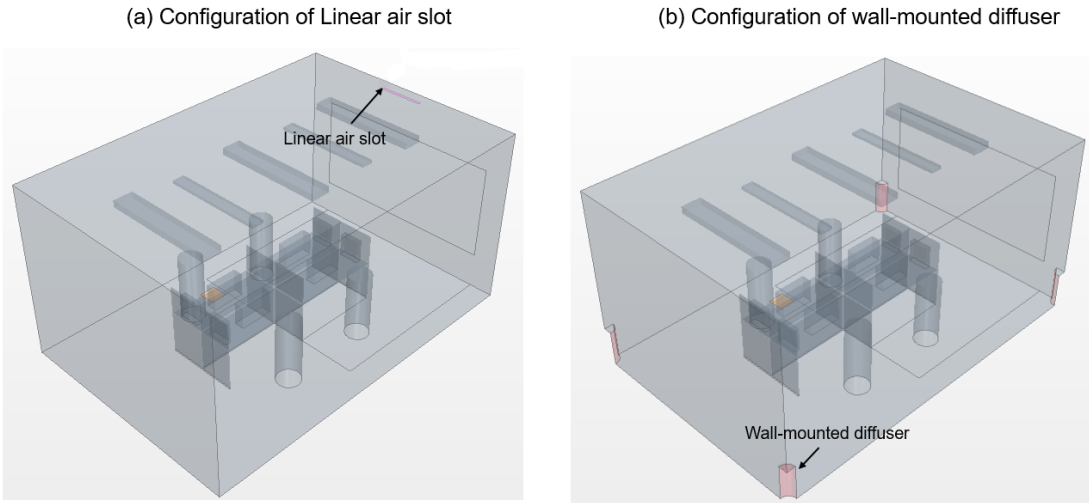

Figure 2-7. Configurations of cases with linear slot diffuser and wall-mounted diffusers: (a) linear slot diffuser; (b) wall-mounted diffusers

3) PCB Cooling Output: PCB cooling output between 100 W to 250 W per each chilled beam was simulated based on the manufacturer data. We considered cases with 100, 150, 200 W (i.e. 13, 19, 25 W/m^2) for MV system (case 1-3), and cases with 100, 125, 150, 175, 200, 225, 250 W (i.e. 13, 16, 19, 22, 25, 28, 31 W/m^2) for DV system (case 5-11) to find the relationship between PCB cooling output and airflow distribution.

4) Supply Air Temperature: As DV system can employ higher supply air temperature compared with MV system, this study examines different supply air temperature ranging from 17 ℃ to 20 ℃ (case 11-14) to see its connection to the system performance.

5) Heat Source Arrangement: Asymmetric load intensity and arrangements are compared to the standard of the symmetric model. In the standard model, two rows of four occupants are equally placed on both sides of the middle office desk (Arr_0). In one asymmetric configuration,

one row of four occupants are all spaced on one side (Arr_1). In the other one, two rows of four occupants are placed asymmetrically across the office desk (Arr_2). Figure 2-8 shows these two configurations and the original model. The PCB cooling output is kept at a constant value of 150 W for each PCB (*i.e.* 19 W/m^2).

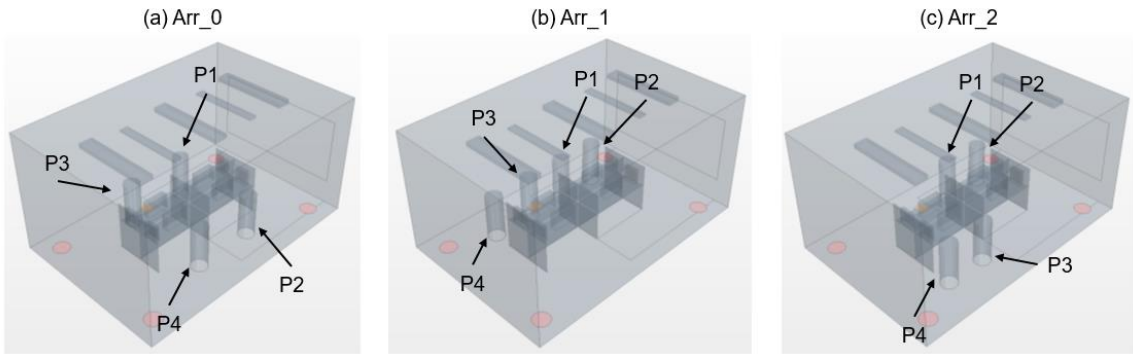

Figure 2-8. Original symmetric and two asymmetric arrangements of indoor occupants with numbered occupants: (a) Arr_0; (b) Arr_1; (c) Arr_2

Evaluating variables

To evaluate the air conditioning performance, four variables are examined with corresponding criteria, including temperature, air velocity, draft rate (DR) and air change effectiveness (ACE). The mean values of all variables are calculated within the breathing zone, which is defined as the space between planes 75 and 1800 mm above the floor and more than 600 mm from the walls or fixed air-conditioning equipment [18].

Air temperature is investigated from two aspects: the mean air temperature and vertical temperature difference. To meet the requirement of comfort zone defined by ASHRAE [18], the mean air temperature should fall in the range from 23 to 26 °C. On the other hand, the vertical temperature difference between head (1.1 m above the floor) and ankles (0.1 m above the floor) is

checked to see if the value is less than 2.6 °C, standing for a 5% dissatisfied due to vertical air temperature difference.

The mean air velocity and DR are used to assess thermal comfort. DR is a predicted percentage of people dissatisfied due to annoyance by draft. The sensation of draft depends on the speed of air, how much the air speed is fluctuating (turbulence), the air temperature and clothing conditions [4]. According to ASHRAE [18], the percentage dissatisfied due to local discomfort from draft should be less than 20%. Also, it is recommended that the air speed for office room is no more than 0.19 m/s in cooling condition when DR is 20% [12]. DR can be calculated, using local air temperature (t, °C), local air velocity (v, m/s) and turbulent kinetic energy (k, J/kg) as Equation (2-3) shows:

$$DR = (34 - \mathrm{t}) \cdot (\mathrm{v} - 0.05)^{0.62} \cdot (37\sqrt{\frac{2}{3}k} + 3.14) \tag{2-3}$$

ACE is calculated based on age-of-air. The age-of-air at a specific location is the average time elapsed since the air at that location entered the space. ACE is defined as the ratio of the age-of-air that would occur with perfect mixing to the actual age-of-air in a considered zone, and the age-of-air with perfect mixing is identical to the average age-of-air in the exhaust outlet [16]. A higher ACE value indicates that the room has fresher air. For a room with ceiling supply of cool air (MV), the value of ACE in breathing zone is generally 1; for a room with floor supply of cool air and ceiling return (DV), it is 1.2.

Chapter 3

Results and Discussion

Using the CFD model and research methods mentioned in Chapter 2, the DV system is firstly validated by existing experiment. Then cases for parametric analyses are verified to determine if the simulations are numerically correct, and compared to find the effect of different parameters.

CFD verification

The CFD model verification assures mass and energy balance in the simulation domain as well as grid convergence. Table 3-1 shows an example of the results for case 7. For all simulated cases, the percentage difference between supply and exhaust air flow rate is lower than 0.1%, while percentage difference between total removal of heat and the total heat load in the office space is also within 0.1%. The results demonstrate that the solution satisfies mass & energy conservation in the simulation domain.

Table 3-1. Calculation of mass and energy conservation

Mass conservation	Supply air flow rate ($\times 10^{-2}$ kg/s)		Exhaust air flow rate ($\times 10^{-2}$ kg/s)	Percentage difference (%)
	9.74		9.75	0.1
Energy conservation	Total removed heat (W)		Total heat load (W)	Percentage difference (%)
	Ventilation	PCB	1402	0.1
	951	450		

For the verification of grid convergence, simulation results for three grid sizes (0.02m, 0.06m, 0.1m) are analyzed. Table 3-2 shows the calculated GCI for these three grid resolutions. It is found that numerical uncertainty due to grid discretization decrease from 16.65% to 4.99% as

the grid size is refined from 0.1 m to 0.02 m. Based on Equation (2-2), the order of accuracy, *p*, is calculated as 1.2. This result indicates that the grid size of 0.02 m, that corresponds to the total cell number of 890,000, can produce a grid-independent solution of velocity distribution near the occupants.

Table 3-2. Calculation of Grid Convergence Index (GCI) for three grid resolutions

Smallest grid size (m)	**0.02**	**0.06**	**0.1**
Number of Cells	890285	210172	166152
Grid refinement factor		3.00	1.67
Avg. velocity magnitude for the 8 L volume located 20 cm above the head (m/s)	0.064	0.071	0.079
GCI		4.99	16.65

Impact of ventilation strategies

Figures 3-1 (a)-(b) show the temperature distribution of the room with combined PCB-MV and PCB-DV system. Despite the effect of the PCB, the characteristics of both ventilation strategies are still reserved: the air in the breathing zone is well mixed with a uniform temperature distribution for MV, whereas a vertical temperature gradient occurs in the DV system. As a result, the vertical temperature difference for the PCB-DV system is 3 °C higher than that of the PCB-MV system, as shown in Table 3-3. A paper by Lin et al. [23] studied the thermal comfort of MV and DV systems (not combined with additional cooling equipment such as PCB) in an office room, and they found a similar pattern that the temperature difference for the DV system between the head and foot level of a sedentary occupant was almost 3 °C. This value is lower than the value simulated in this study (4 °C) even with the effect of PCB. This difference is likely due to the larger heat load (120 W/m^2) with a smaller air change rate (1.5 h^{-1}) compared to this study (58.5 W/m^2, 4 h^{-1}). Comparing PCB-DV and PCB-MV, the PCB-DV system achieves a much

lower mean temperature (23.09 °C) in the breathing zone under the same conditions of air change rate and PCB cooling output. In the case of PCB-MV, temperature is generally higher near the window than the PCB-DV system, suggesting that underfloor diffusers can remove heat more efficiently in the areas close to the window.

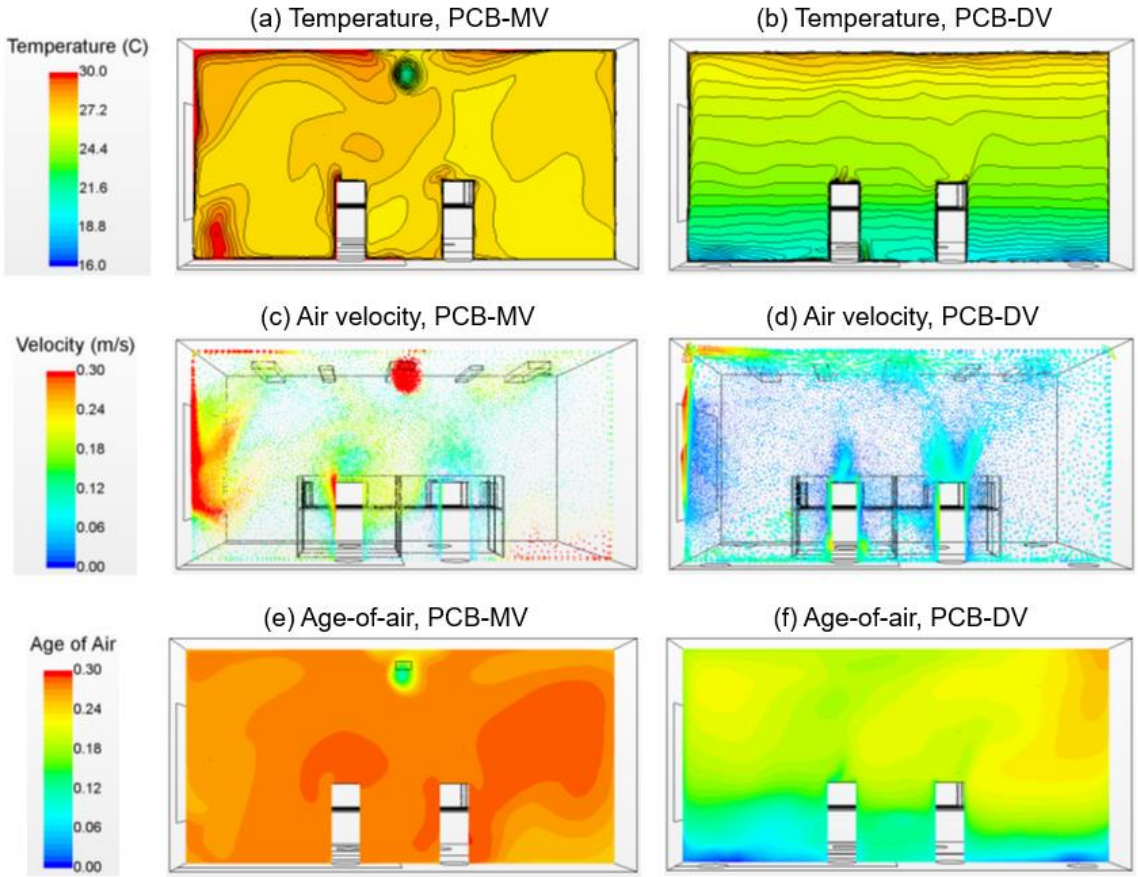

Figure 3-1. Performance of the combined PCB-DV system with different ventilation strategies: (a) temperature, PCB-MV; (b) temperature, PCB-DV; (c) air velocity, PCB-MV; (d) air velocity, PCB-DV; (e) age-of-air, PCB-MV; (f) age-of-air, PCB-DV

Figures 3-1 (c)-(d) show the velocity distributions. For both PCB-MV and PCB-DV systems, non-uniform and high velocity (larger than 0.19 m/s) occurs near the occupant simulators. Also, high air velocity occurs near the window with the MV system mainly due to the

air jet moving along the ceiling and opposite wall that keeps air velocity high near the wall and window. For the PCB-DV system, high air velocity mostly occurs near the occupant simulators. This pattern is similar to the situation described in the paper by Lin et al. [23]. Though the DV system helps a reduction of 58% in mean velocity and 61% in DR compared to the MV system, the values are acceptable since they are lower than the set limit (0.19 m/s and 20%).

Figures 3-1 (e)-(f) show age of air distributions. The range of age of air in the breathing zone is generally lower with the PCB-DV system (0-10 minutes) than the PCB-MV system (17-18 minutes), thereby resulting in 40% higher ACE with the PCB-DV system. The higher ACE reflects a better ventilation performance with the PCB-DV system. This result is in accordance with the previous study conducted by Lin et al. [24] that compared the contaminate concentration between MV and DV systems. It showed lower concentrations of carbon dioxide, toluene, benzene, formaldehyde in the breathing zone with the DV system.

Table 3-3. Calculated variables of the combined PCB-MV and PCB-DV system

Case	**Ventilation method**	**Mean temp. (°C)**	**Mean velocity (m/s)**	**Vertical temp. difference (°C)**	**DR (%)**	**ACE**
2	MV	27.25	0.12	0.55	5.94	0.93
7	DV	23.09	0.05	3.89	2.29	1.56

Impact of supply air diffuser type

Figure 3-2 and Table 3-4 describe ventilation performance of the combined PCB-MV system with 1) sidewall grille and 2) linear slot diffuser. The temperature (Figures 3-2 (a)-(b)) is fairly uniform for both cases with the temperature difference within 1 °C in the breathing zone; however, the mean temperature is almost 2 °C lower in the case with the linear slot diffuser. Figures 3-2 (c)-(d) reveal that with the linear slot diffuser, the air velocity decreases near the

window while increasing at the ground level. The reason of the decreased air velocity near the window is that the air jet from the linear slot diffuser offsets the buoyant air flow from the heated window surface. The mean velocity and draft rate are very close for both diffusers. According to Figure 3-2 (e)-(f), the linear slot diffuser provides fresher air in the whole room space, considering that age-of-air is about 3 minutes smaller while the ACE increases 18% compared to the sidewall diffuser. Previous studies [25, 26] investigated experimentally and numerically the effects of different supply air diffuser types in MV on indoor air contaminant concentrations and found that ceiling inlets could produce higher ventilation effectiveness compared to a wall diffuser regardless of the type of ceiling inlet.

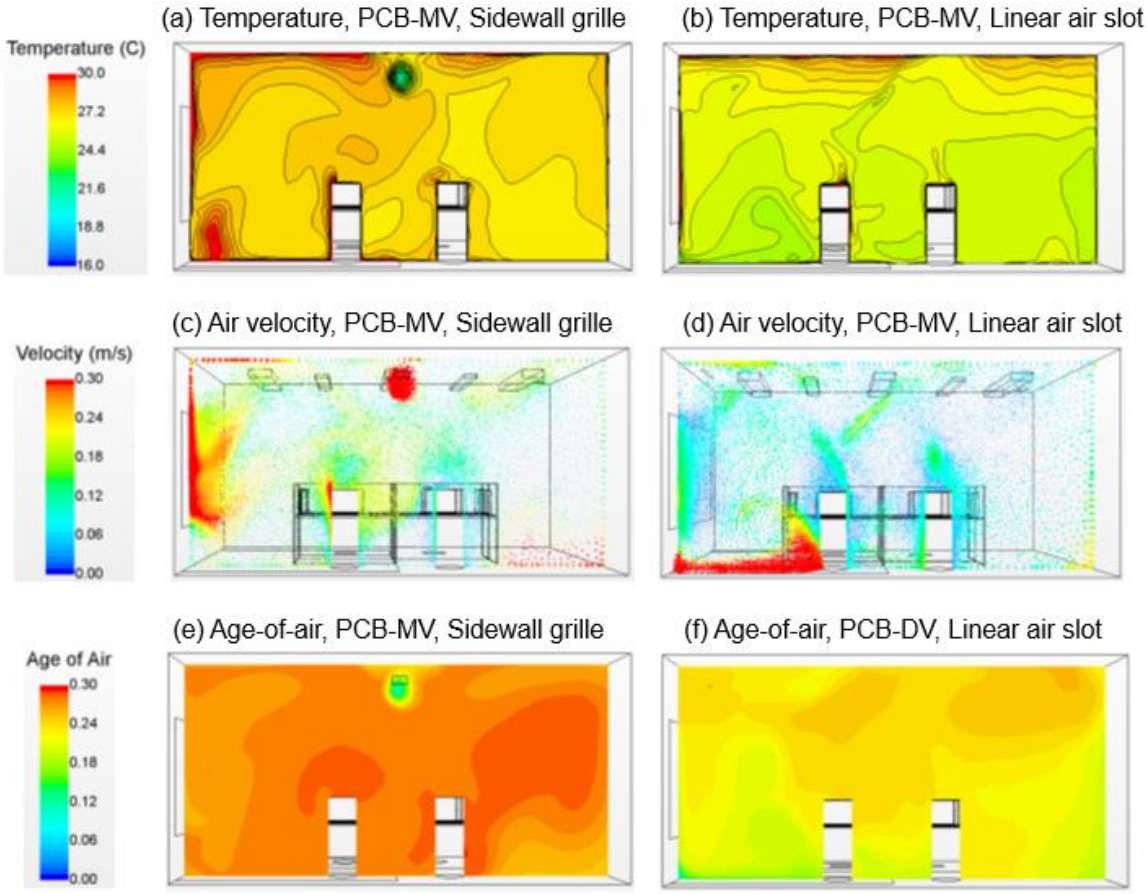

Figure 3-2. Performance of the combined PCB-MV system with different types of supply air diffuser: (a) temperature, PCB-MV, sidewall grille; (b) temperature, PCB-MV, linear slot diffuser; (c) air velocity, PCB-MV, sidewall grille; (d) air velocity, PCB-MV, linear slot diffuser; (e) age-of-air, PCB-MV, sidewall grille; (f) age-of-air, PCB-MV, linear slot diffuser

Figure 3-3 and Table 3-4 show the system performance of the combined PCB-DV system with the underfloor diffusers and wall-mounted displacement ventilation diffusers. The patterns of temperature, velocity and age-of-air distribution for both cases are similar. Compared to the underfloor diffuser, the wall-mounted diffuser can achieve 0.75 °C lower vertical temperature difference and 13% higher ACE, as the supply air from the diffusers flows toward the occupants and strengthen the thermal plume effect. The difference in mean temperature between these two diffusers is within 3% and the mean velocity and DR are lower than the set limit (0.19 m/s and 20%). This result is different from the study by Zhang et al. [10], where the wall-mounted diffuser had a very close performance to the perforated-panel on the floor (with a similar geometry and supply air velocity with the floor-supply diffuser used in this study). The possible reason for the difference may be that the air change rate for the perforated-panel case (8.62 h^{-1}) was larger than the quarter-circular-perforated diffuser case (4.57 h^{-1}) while in this study the air change rate is the same for all cases (4 h^{-1}).

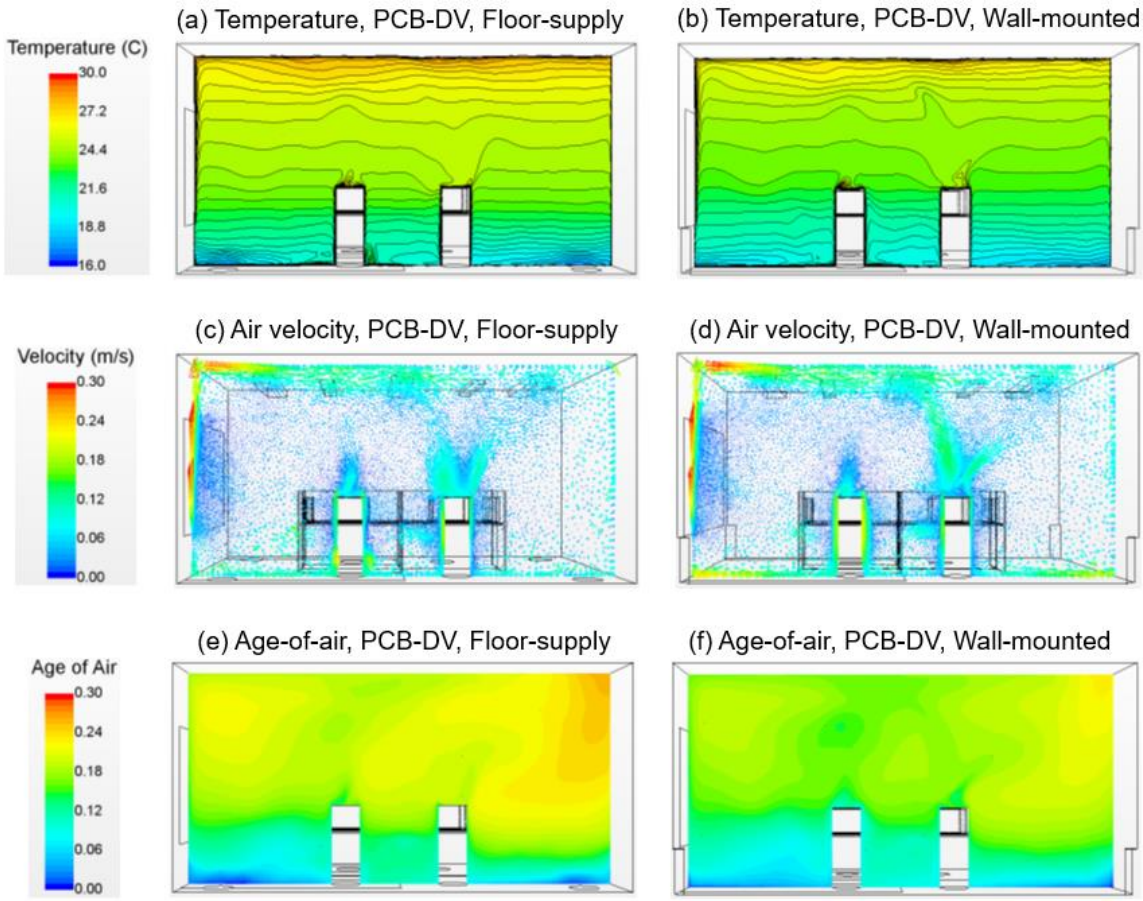

Figure 3-3. Performance of the combined PCB-DV system with different types of supply air diffuser: (a) temperature, PCB-DV, floor-supply diffusers; (b) temperature, PCB-DV, wall-mounted diffusers; (c) air velocity, PCB-DV, floor-supply diffusers; (d) air velocity, PCB-DV, wall-mounted diffusers; (e) age-of-air, PCB-DV, floor-supply diffusers; (f) age-of-air, PCB-DV, wall-mounted diffusers

Table 3-4. Calculated variables of the PCB-DV and PCB-MV systems with different types of supply air diffuser

Case	Ventilation method	Air supply diffuser type	Mean temp. (°C)	Mean velocity (m/s)	Vertical temp. difference (°C)	DR (%)	ACE
2	MV	Sidewall grille	27.25	0.12	0.55	5.94	0.93
4	MV	Linear air slot	25.43	0.10	0.54	5.85	1.14
12	DV	Floor-supply diffusers	23.09	0.05	3.89	2.29	1.56
15	DV	Wall-mounted diffusers	22.34	0.05	3.47	2.61	1.79

Impact of PCB cooling output

Figure 3-4 illustrates the variation of temperature distribution and ventilation performance with increasing PCB cooling output for the combined PCB-MV system. Figure 3-4 (a) shows the thermal performance of the PCB-MV system. With the increase of PCB cooling output from 13 W/m^2 to 25 W/m^2, the mean temperature in the breathing zone decreases by 2.40 °C while the vertical temperature difference changes a little and stays around ±0.5 °C. This result suggests evenly mixed air in the breathing zone for the MV system.

For the velocity distribution, the values of the mean velocity and DR change minimally with increased PCB cooling output, as shown in Figure 3-4 (b). Even though the mean velocity and DR of the MV system are much higher than those of the DV system (shown in Figure 3-5 (b)), they are still within the acceptable range based on the criteria used in this study (less than 0.19 m/s and 20%).

In terms of the ventilation effectiveness as indicated in Figure 3-4 (c), a larger PCB cooling output seems to have minor effect on the age-of-air and ACE. The mean age-of-air goes up slightly with the increasing PCB cooling output, probably because the downward air flow from the PCB impedes the old air from escaping the room. The calculated ACE of each case is close to 1, indicating fairly uniform air mixing with ceiling supply of cool air (MV).

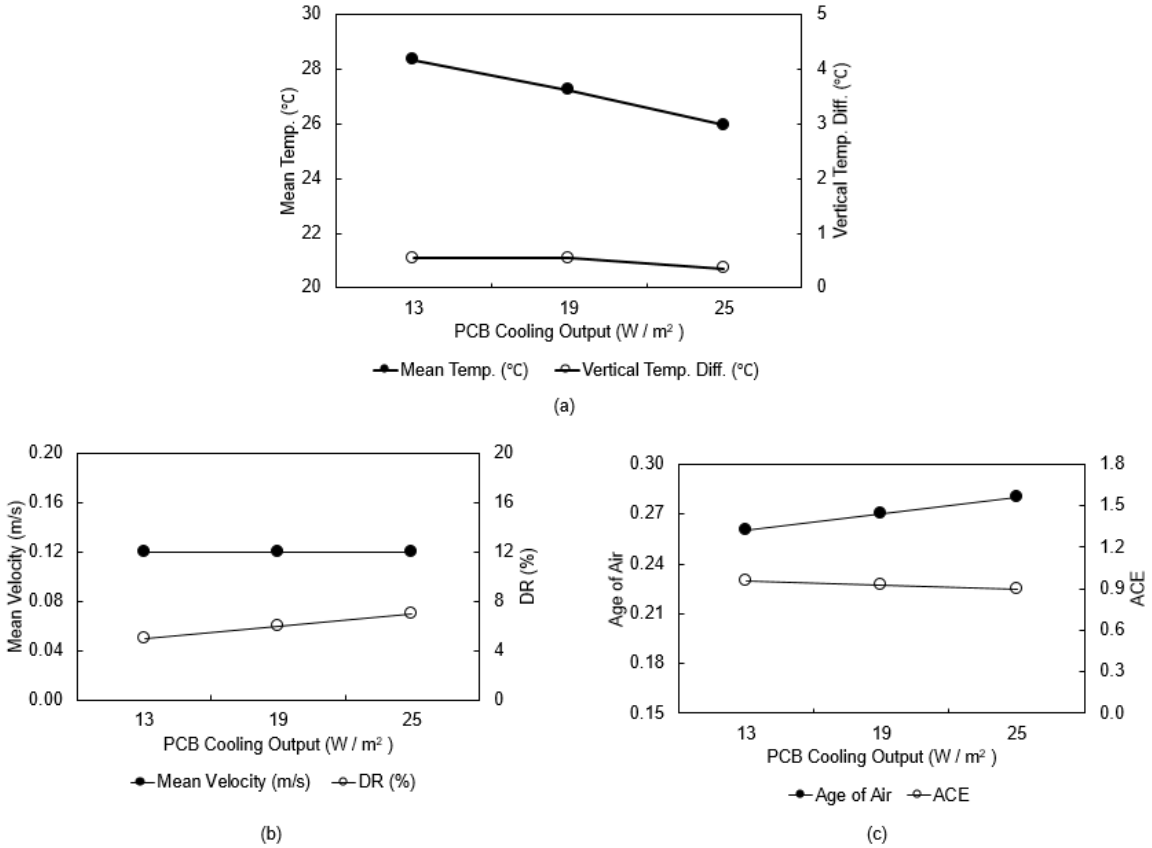

Figure 3-4. Performance of the combined PCB-MV system with different PCB cooling output: (a) Mean temp. & Vertical temp. diff. vs. PCB cooling output; (b) Mean velocity & DR vs. PCB cooling output; (c) Age of air & ACE vs. PCB cooling output

Figure 3-5 (a) shows the thermal variables of combined PCB-DV system with different PCB cooling output. In this case, the mean air temperature in the breathing zone and the vertical temperature difference notably decrease with the increase of the PCB cooling output. This illustrates that a larger PCB cooling output (45-55% total cooling load) can reduce the vertical temperature gradient but may also cause overcooling in the occupied zone. This result suggests that the increasing PCB cooling output in DV can result in restriction of the large vertical temperature gradient, which is one undesired characteristic inherited from DV. For the cases with 4 h^{-1} ACH and 17 °C supply temperature, it may be difficult to simultaneously achieve the temperature of the comfort zone and the acceptable vertical temperature difference. It is also

found that the air temperature is more evenly distributed with the increase of PCB cooling output, reflecting increased air mixing with large PCB cooling output.

Figure 3-5 (b) illustrates that a larger PCB cooling output promotes air velocity and leads to a higher sensation of drafts in the breathing zone. This pattern is mainly because of the air draft toward the breathing zone caused by the PCB. However, the mean velocity and DR still fall in the acceptable range (less than 0.19 m/s and 20%) when the PCB cooling output increases greatly from 13 W/m^2 to 31 W/m^2. The control of indoor air distribution comes to a minor priority in the design of the combined PCB-DV system.

As indicated in Figure 3-5 (c), the age-of-air increases with higher PCB cooling output. The ACE decreases because of the impedance of more downward drafts. The ACE decreases by 25% when the PCB cooling output changes from 13 W/m^2 to 31 W/m^2. It could be predicted that when the PCB cooling output exceeds 250 W, the ACE would be lower than 1.2 and more close to 1.0. This proves that a larger PCB cooling output disrupts the original properties of DV and yield uniform air distribution similar to an MV system.

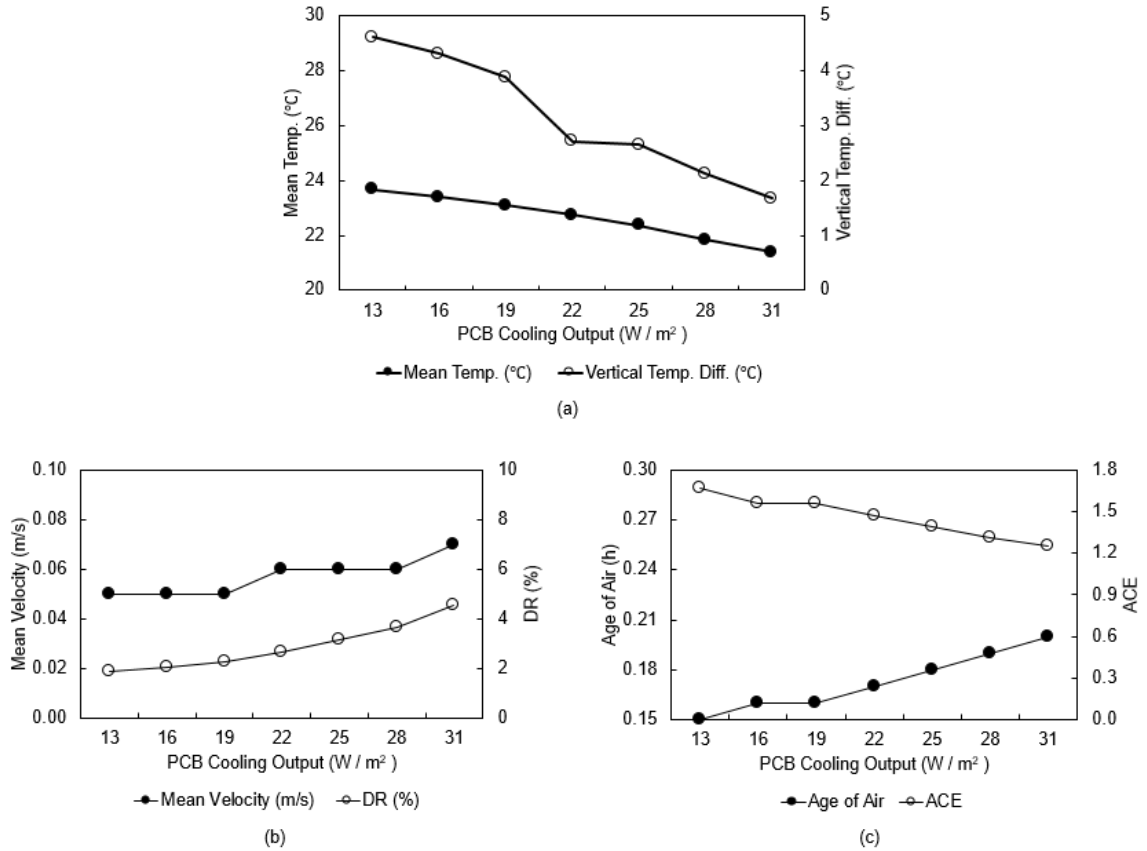

Figure 3-5. Performance of the combined PCB-DV system with different PCB cooling output: (a) Mean temp. & Vertical temp. diff. vs. PCB cooling output; (b) Mean velocity & DR vs. PCB cooling output; (c) Age of air & ACE vs. PCB cooling output

Impact of supply air temperature

Figure 3-6 shows how the temperature distribution and ventilation performance of the PCB-DV system varies with different supply air temperature. The variated supply air temperature seems to have marginal effect on vertical temperature gradient, velocity distribution and ventilation effectiveness, except for the mean temperature. The mean temperature goes up from 23.09 ℃ to 26.11 ℃ when the supply air temperature varies from 17 ℃ to 20 ℃. The relationship is straightforward as higher-temperature supply air heats up the indoor environment, leading to an increase of temperature. This result suggests the increase of supply air temperature

can enhance the mean temperature in the breathing zone while keeping the other parameters constant, which is a good solution to satisfying the criteria of mean temperature and vertical temperature gradient simultaneously. In a previous study by Xu and Kotani [28], experiments were conducted to measure the temperature gradient and the ventilation efficiency in a room ventilated by DV with different supply air temperature. It was observed that the vertical temperature difference between head (1.1 m above the floor) and ankles (0.1 m above the floor) decreased only by 1 °C while vertical distribution of contaminant concentration almost kept constant when the supply temperature varied from 20 °C to 25 °C.

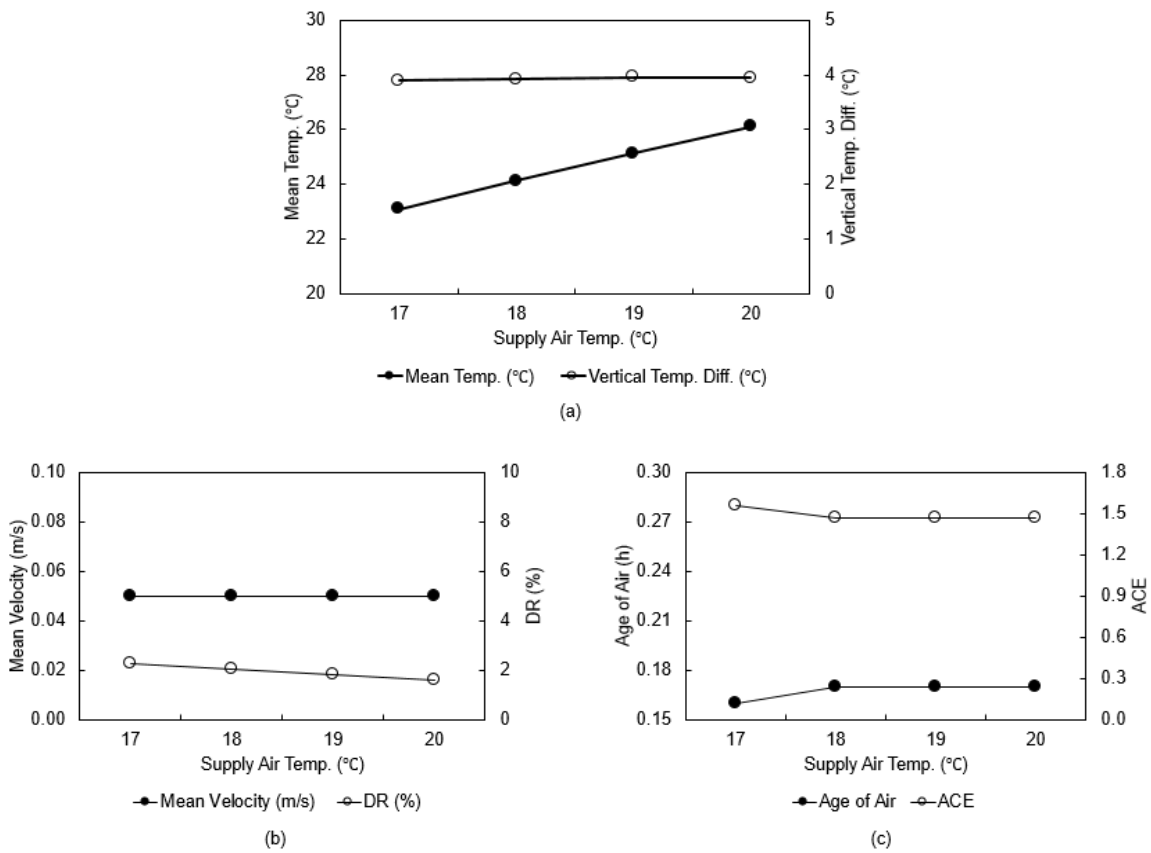

Figure 3-6. Performance of the combined PCB-DV system with different supply air temperature: (a) Mean temp. & Vertical temp. diff. vs. PCB cooling output; (b) Mean velocity & DR vs. PCB cooling output; (c) Age of air & ACE vs. PCB cooling output

Impact of heat source arrangement

The effect of different arrangements of heat loads on thermal and ventilating performance is studied under the same PCB cooling output and heat load intensity. The results are shown in Figure 3-7 and Table 3-5. Though the distribution of each variable is a little different for each arrangement, the air stratification and calculated values in the breathing zone don't change a lot (less than 5%) except for ACE. From the table, it can be observed that the two asymmetric arrangements own 6% lower ACE than the symmetric one. Except for the simulation error, the lower air quality may be attributed to inadequate effect from the displacement ventilation system, as some of the diffusers are far away from the occupants in both asymmetric cases.

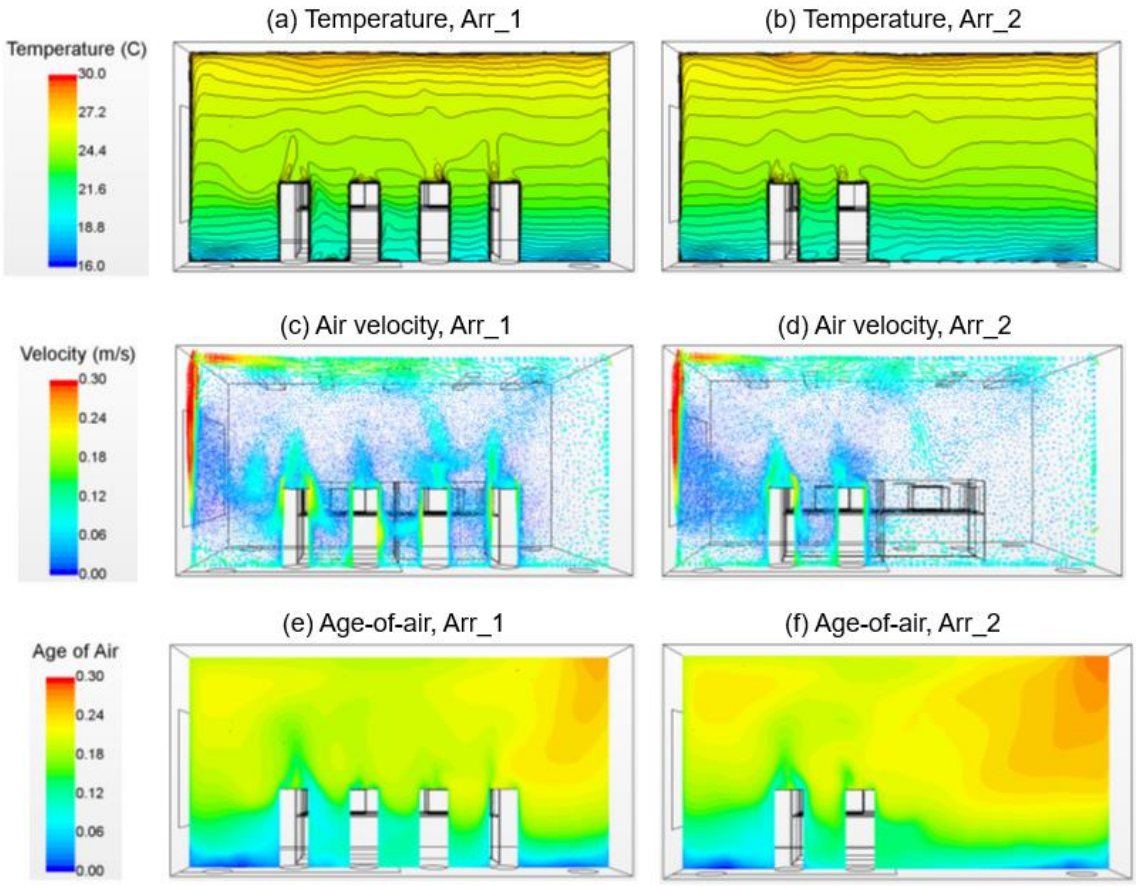

Figure 3-7. Performance of the combined PCB-DV system with different occupants' arrangements: (a) temperature, Arr_1; (b) temperature, Arr_2; (c) air velocity, Arr_1; (d) air velocity, Arr_2; (e) age-of-air, Arr_1; (f) age-of-air, Arr_2

Table 3-5. Calculated variables of the PCB-DV system with different occupants' arrangements

Case	**Load arrangement**	**Mean temp. (°C)**	**Mean velocity (m/s)**	**Vertical temp. difference (°C)**	**DR (%)**	**ACE**
7	Arr_0	23.09	0.05	3.89	2.29	1.56
16	Arr_1	23.1	0.05	3.88	2.28	1.47
17	Arr_2	23.09	0.05	3.87	2.31	1.47

Chapter 4

Conclusion

In this paper, the validated and verified CFD simulations are performed to determine the temperature distribution, velocity distribution and ventilation effectiveness of the combined PCB-DV system. The study conducts a detailed analysis of the performance of the PCB-DV system by focusing on the impacts of five variables: 1) ventilation strategy; 2) supply air diffuser; 3) PCB cooling output; 4) supply air temperature; 5) internal heat source arrangement. The following conclusions are obtained:

• Compared to the PCB-MV system, the PCB-DV system yields air stratification. Under the same PCB cooling output, heat load and ACH, the PCB-DV system achieves 3 ℃ lower mean air temperature and 3 ℃ greater vertical temperature gradient than the PCB-MV system. The large vertical temperature gradient may result in thermal discomfort. Nonetheless, the PCB-DV system yields a 60% lower draft risk and a 40% higher ACE in the breathing zone, reflecting a better indoor air distribution and air quality.

• Supply air diffuser type has distinct effect on the system performance for both PCB-DV and PCB-MV system. For the MV cases, both the linear air slot and side grille show rather evenly-distributed temperature in the breathing zone and high velocity of air in the vicinity of the occupants. The linear slot diffuser helps achieve 3 ℃ lower mean air temperature and 18% higher ACE than the sidewall grille. For the DV cases, the temperature distribution, velocity distribution and age-of-air distribution are similar for the underfloor diffusers and wall-mounted diffusers. The wall-mounted diffusers give 11 % lower vertical temperature difference and 13% higher ACE.

• The PCB cooling output only affects the mean temperature for the PCB-MV system while it acts as an important factor for the air distribution in the PCB-DV system. When PCB cooling output assumes 50% total cooling load, the vertical temperature difference for the PCB-DV system is restricted below 2.6 ℃. But at the same time, the mean air temperature starts to exceed the lower limit, 23 ℃. It is difficult to find a situation satisfying both criteria of mean temperature and vertical temperature difference in this study with fixed room configuration, heat load and supply air condition (ACH 4 h^{-1} and supply air temperature 17 ℃). The ACE decreases by 25% when the PCB cooling output changes from 13 W/m^2 to 31 W/m^2.

• Supply air temperature only has notable influence on the mean temperature for the PCB-DV system. A higher supply air temperature leads to a higher mean temperature while the other parameters almost keeps constant, contributing to a 3 ℃ increase of mean temperature when the supply air temperature changes from 17 ℃ to 20 ℃. This gives insights that optimal operation for the combined PCB-DV system in an office room may be achieved when the PCB assumes 50% total cooling output with an enhanced supply air temperature of 19-20 ℃.

• Different load arrangements (occupant simulators in this study) seem to have marginal impact on the performance of the PCB-DV system based on temperature distribution and velocity distribution, and minor influence on ventilation effectiveness.

Chapter 5

Limitation and Future Work

In this paper, parametric analyses are conducted to study the performance of combined PCB-DV systems with different parameters. It should be noticed that this study only discussed how the variation of different parameters would affect the performance of combined PCB-DV systems, but didn't delve into how this system would be actually operated. When the combined PCB-DV system is operated in a thermostat-controlled space, relevant parameters (e.g. ACH, supply air temperature, chilled water supply temperature) are controlled to maintain right temperature in the breathing zone. Figuring out the control strategies of relevant parameters can be helpful to design this combined system properly.

The model validation is only conducted for DV system instead of the combined PCB-DV system due to lack of available experiments. Future work can proceed on the establishment of experiments for the performance evaluation of combined PCB-DV systems to determine a more accurate model as a representation of the real situation.

Furthermore, humidity is not considered in this paper. When the combined PCB-DV system is chosen as the air-conditioning system, it is important for designers to control the indoor humidity level so that the condensation on the surface of beams can be avoided, because no drain pan or pipe is attached on the PCB to deal with condensation. Further work can concentrate on the humidity control of the combined PCB-DV systems.

Bibliography

[1] Kim, J., 2015. Characterizing the In-Situ Performance of Passive Chilled Beams. *ASHRAE Transactions*, *121*, p.1N.

[2] Riffat, S.B., Zhao, X. and Doherty, P.S., 2004. Review of research into and application of chilled ceilings and displacement ventilation systems in Europe. *International Journal of Energy Research*, *28*(3), pp.257-286.

[3] O'Rourke, M., 2008. Design considerations for active chilled beams. *ASHRAE Journal*, *50*(9), p.50.

[4] Kosonen, R., Saarinen, P., Koskela, H. and Hole, A., 2010. Impact of heat load location and strength on air flow pattern with a passive chilled beam system. *Energy and Buildings*, *42*(1), pp.34-42.

[5] Fredriksson, J. and Sandberg, M., 2009. The effect of false ceiling on the cooling capacity of passive chilled beams. *Building and Environment*, *44*(7), pp.1426-1430.

[6] Nelson, I.C., Culp, C.H., Rimmer, J. and Tully, B., 2016. The effect of thermal load configuration on the performance of passive chilled beams. *Building and Environment*, *96*, pp.188-197.

[7] Lau, J. and Chen, Q., 2007. Floor-supply displacement ventilation for workshops. *Building and Environment*, *42*(4), pp.1718-1730.

[8] Kobayashi, N. and Chen, Q., 2003. Floor-supply displacement ventilation in a small office. *Indoor and Built Environment*, *12*(4), pp.281-291.

[9] Gilani, S., Montazeri, H. and Blocken, B., 2016. CFD simulation of stratified indoor environment in displacement ventilation: Validation and sensitivity analysis. *Building and Environment*, *95*, pp.299-313.

[10] Zhang, T.T., Lee, K. and Chen, Q.Y., 2009. A simplified approach to describe complex diffusers in displacement ventilation for CFD simulations. *Indoor Air*, *19*(3), pp.255-267.

[11] Chen, Q. and Srebric, J., 2002. A procedure for verification, validation, and reporting of indoor environment CFD analyses. *HVAC&R Research*, *8*(2), pp.201-216.

[12] Koskela, H., Häggblom, H., Kosonen, R. and Ruponen, M., 2010. Air distribution in office environment with asymmetric workstation layout using chilled beams. *Building and Environment*, *45*(9), pp.1923-1931.

[13] Peric, M. and Ferguson, S., 2005. The advantage of polyhedral meshes. *CD-adapco< http://www. cd-adapco. com/press_room/dynamics/24/testVspoly. html*.

[14] Bolashikov, Z.D., Melikov, A.K., Rezgals, L., Lipczynska, A., Mustakallio, P., Kosonen, R. and Aho, I., 2014. Comparison of radiant and convective cooling of office room: effect of workstation layout. *In 13th International Conference on Indoor Air Quality and Climate*.

[15] Mustakallio, P., Bolashikov, Z., Kostov, K., Melikov, A. and Kosonen, R., 2016. Thermal environment in simulated offices with convective and radiant cooling systems under cooling (summer) mode of operation. *Building and Environment*, *100*, pp.82-91.

[16] Salim, S.M. and Cheah, S., 2009. Wall Y strategy for dealing with wall-bounded turbulent flows. In *Proceedings of the International MultiConference of Engineers and Computer Scientists*, *Hong Kong* (Vol. 2).

[17] Celik, I.B., Ghia, U. and Roache, P.J., 2008. Procedure for estimation and reporting of uncertainty due to discretization in {CFD} applications. *Journal of fluids {Engineering-Transactions} of the {ASME}*, *130*(7).

[18] Standard, ASHRAE, 2010. Standard 55-2010:“Thermal Environmental Conditions for Human Occupancy”; ASHRAE. *Atlanta* USA.

[19] Standard, ASHRAE, 129 (1997) (RA 2002) “Measuring air change effectiveness” American Society of Heating, Refrigerating and Air-Conditioning Engineers.

[20] Standard, A.S.H.R.A.E., Standard 62.1-2010 (2010). ventilation for acceptable indoor air quality, Atlanta, GA. *American Society of Heating, Refrigerating and Air-Conditioning Engineers, Inc*.

[21] Rim, D. and Novoselac, A., 2010. Occupational exposure to hazardous airborne pollutants: Effects of air mixing and source location. *Journal of occupational and environmental hygiene*, *7*(12), pp.683-692.

[22] Rim, D. and Novoselac, A., 2010. Ventilation effectiveness as an indicator of occupant exposure to particles from indoor sources. *Building and Environment*, *45*(5), pp.1214-1224.

[23] Lin, Z., Chow, T.T., Fong, K.F., Wang, Q. and Li, Y., 2005. Comparison of performances of displacement and mixing ventilations. Part I: thermal comfort. *International journal of refrigeration*, *28*(2), pp.276-287.

[24] Lin, Z., Chow, T.T., Fong, K.F., Tsang, C.F. and Wang, Q., 2005. Comparison of performances of displacement and mixing ventilations. Part II: indoor air quality. *International Journal of Refrigeration*, *28*(2), pp.288-305.

[25] Lee, E., Khan, J.A., Feigley, C.E., Ahmed, M.R. and Hussey, J.R., 2007. An investigation of air inlet types in mixing ventilation. *Building and environment*, *42*(3), pp.1089-1098.

[26] Khan, J.A., Feigley, C.E., Lee, E., Ahmed, M.R. and Tamanna, S., 2006. Effects of inlet and exhaust locations and emitted gas density on indoor air contaminant concentrations. *Building and Environment*, *41*(7), pp.851-863.

[27] Ariff, M., Salim, S.M. and Cheah, S.C., 2009, December. Wall y+ approach for dealing with turbulent flow over a surface mounted cube: part 1—low Reynolds number. In *Seventh International Conference on CFD in the Minerals and Process Industries* (pp. 1-6).

[28] Xu, M. and Kotani, H., 2001. Vertical profiles of temperature and contaminant concentration in rooms ventilated by displacement with heat loss through room envelopes. *Indoor Air*, *11*(2), pp.111-119.

Appendix A

STAR-CCM+ Settings

(a) Mesh setting for sensitive regions

Mesh Values	
Surface Size	
Relative/Absolute	Relative to base
Size Method	Min and Target
Relative Minimum Size	
Percentage of Base	10.0
Absolute Size	0.01 m
Relative Target Size	
Percentage of Base	20.0
Absolute Size	0.02 m

(b) Mesh setting for other regions

Surface Size	
Relative/Absolute	Relative to base
Size Method	Min and Target
Relative Minimum Size	
Percentage of Base	25.0
Absolute Size	0.025 m
Relative Target Size	
Percentage of Base	100.0
Absolute Size	0.1 m

Figure A-1. Mesh setting: (a) sensitive regions; (b) other regions

(a) Mesh model

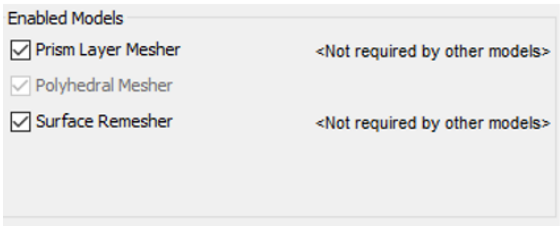

(b) Physical model

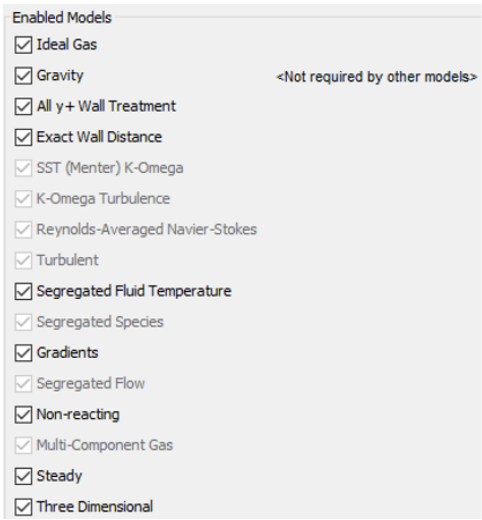

Figure A-2. Mesh and physical model used for simulation: (a) mesh model; (b) physical model

(a) Gas composition

(b) Initial condition

(c) Species Source of SF_6

Figure A-3. Multi-component gas setting for SF_6 and air: (a) gas composition; (b) initial condition; (c) species source of SF_6

(a) Indoor heat sources

Type	Wall
Thermal Specification	
Condition	Heat Source
Heat Source	
Method	Constant
Value	31.5 W
Dimensions	Power

(b) Heated building enclosure

Type	Wall
Thermal Specification	
Condition	Heat Flux
Heat Flux	
Method	Constant
Value	3.76 W/m^2
Dimensions	Power/Length^2

(c) Supply air outlet

Type	Velocity Inlet
Velocity Specification	
Method	Magnitude + Direction
Species Mole Fraction	
Method	Constant
Value	[1.0, 0.0]
Dimensions	Dimensionless
Static Temperature	
Method	Constant
Value	17.0 C
Dimensions	Temperature
Turbulence Intensity	
Method	Constant
Value	0.01
Dimensions	Dimensionless
Turbulent Viscosity Ratio	
Method	Constant
Value	10.0
Dimensions	Dimensionless
Velocity Magnitude	
Method	Constant
Value	0.16 m/s
Dimensions	Velocity

Figure A-4. Boundary conditions: (a) indoor heat sources; (b) heated building enclosure; (c) supply air outlet

Appendix B

Calculation of Order of Accuracy p

In this study, the three grid sizes h of the representative cell are 0.02 m (h_1), 0.06 m (h_2) and 0.1 m (h_3). Then the grid refinement factor r is:

$$r_{21} = h_2/h_1 = 0.06\ m/0.02\ m = 3$$

$$r_{32} = h_3/h_2 = 0.1\ m/0.06\ m = 1.67$$

The order of accuracy p can be calculated using the following expressions:

$$p = \frac{1}{\ln(r_{21})}|ln|\varepsilon_{32}/\varepsilon_{21}| + q(p)|$$

$$q(p) = \ln(\frac{r_{21}^p - s}{r_{32}^p - s})$$

$$s = 1 \cdot sgn(\varepsilon_{32}/\varepsilon_{21})$$

Where $\varepsilon_{32} = \phi_3 - \phi_2$, $\varepsilon_{21} = \phi_2 - \phi_1$, and ϕ_k denotes the solution on the kth grid. In this study, ϕ is the average velocity of magnitude for the 8 L sampling volume located 20 cm above the head (m/s). The values of ϕ_1, ϕ_2 and ϕ_3 are 0.064, 0.071 and 0.079 m/s, respectively. Using iteration method, the value of p is calculated as 1.2.